

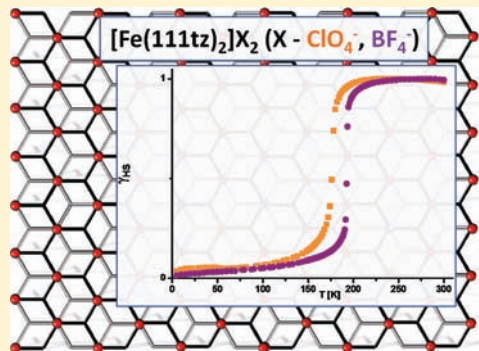
HS \rightleftharpoons LS Transition in Iron(II) Two-Dimensional Coordination Networks Containing Tris(tetrazol-1-ylmethyl)methane As Triconnected Building Block

Agata Białońska, Robert Bronisz,* Mikołaj F. Rudolf, and Marek Weselski*

Faculty of Chemistry, University of Wrocław, F. Joliot-Curie 14, 50-383 Wrocław, Poland

Supporting Information

ABSTRACT: Novel tripodal ligand 1,1',1''-tris(tetrazol-1-ylmethyl)methane (**111tz**) and products of its reactions with perchlorate as well as with tetrafluoroborate salts of iron(II) are presented. The isostructural complexes, $[\text{Fe}(\mathbf{111tz})_2](\text{ClO}_4)_2$ and $[\text{Fe}(\mathbf{111tz})_2](\text{BF}_4)_2$, were isolated as two-dimensional (2D) coordination networks revealing a honeycomb-like pattern with cages occupied by disordered anions. **111tz** molecules act as a tridentate ligand bridging three adjacent Fe(II) ions, and the nitrogen N4 atom of six tetrazole rings (tz) is placed in octahedron vertices of FeN_6 chromophores. The complexes, crystallizing in the $P\bar{3}$ space group, were characterized by variable-temperature single-crystal X-ray diffraction and variable-temperature magnetic susceptibility measurements. Variable-temperature magnetic susceptibility measurements show that both systems undergo abrupt and complete spin transition with $T_{1/2}^{\uparrow} = T_{1/2}^{\downarrow} = 176$ K for perchlorate and $T_{1/2}^{\uparrow} = 193.8$ and $T_{1/2}^{\downarrow} = 192.8$ K for the tetrafluoroborate analogue. Change of spin state in both complexes is accompanied by a thermochromic effect. The HS \rightarrow LS transition in $[\text{Fe}(\mathbf{111tz})_2](\text{ClO}_4)_2$ involves shortening of the Fe–N4 bond lengths from 2.171(2) Å (293 K) to 2.002(1) Å (100 K). In $[\text{Fe}(\mathbf{111tz})_2](\text{BF}_4)_2$, lowering of temperature from 293 to 100 K is accompanied by shortening of the Fe–N4 distances from 2.179(2) to 1.987(2) Å, respectively. Perchlorate in $[\text{Fe}(\mathbf{111tz})_2](\text{ClO}_4)_2$ or tetrafluoroborate anions in $[\text{Fe}(\mathbf{111tz})_2](\text{BF}_4)_2$ are engaged in the formation of intermolecular contacts within as well as with the neighboring 2D layer.



INTRODUCTION

Six coordinated metal ions with electronic configuration $3d^4$ – $3d^7$ in the octahedral environment can be switched between high spin (HS) and low spin (LS) states by external stimuli like change of temperature, pressure, or light irradiation.^{1–6} This phenomenon is called spin crossover (SCO) and is associated with change of magnetic, optical, and dielectric properties. These features make a foundation of potential technological interest of SCO complexes.^{7,8} Fe(II) is the most explored 3d ion constituting switchable materials in which a HS \rightleftharpoons LS transition occurs between paramagnetic high ($t_{2g}^4e_g^2$) and diamagnetic LS state ($t_{2g}^6e_g^0$). In complexes with FeN_6 chromophore, a transfer of two electrons is accompanied by shortening of the metal–ligand bond length at about 0.2 Å. In effect a reduction of the FeN_6 coordination octahedron volume takes place at about 3 \AA^3 .⁹ This structural perturbation influences properties of neighboring molecules as well as it may be elastically propagated along a whole crystal lattice.¹⁰ In monomeric systems¹¹ cooperativity of the spin transition strongly depends on a presence of intermolecular interactions like hydrogen bonds and/or $\pi\cdots\pi$ interactions between molecules.^{12–14} Alternatively, SCO centers may be joined by a system of covalent bonds of bridging ligand molecules.^{15–21} For construction of the SCO coordination polymers, bidentate ligands comprising five or six membered heterocyclic rings as well as cyanometallate anions are frequently used.^{22–26} In a

group of ligands containing azole rings as donor groups: 4-R-1,2,4-triazoles,^{27–30} 1-R-1,2,3-triazoles,³¹ (R = substituent) and derivatives of 1- and 2-substituted tetrazoles are intensively studied.³² Noteworthy, highly cooperative spin transitions in polymeric systems based on 1H,2,4-triazole, 4-amino-1,2,4-triazole molecules or $\text{Pt}(\text{CN})_4^{2-}$ anions were utilized for construction of nanoparticles exhibiting memory effect.³³ Iron(II) complexes with bis(tetrazole)-type ligands crystallize in a form of one- (1D), two- (2D), and three-dimensional (3D) networks revealing a wide variety of their architectures. In the series of complexes based on 1,4-bis(tetrazol-1-yl)butane (btzb),^{15–17} 1,2-bis(tetrazol-1-yl)ethane (endi),¹⁹ 1,2-bis(tetrazol-1-yl)propane (btzp),²⁰ 1,2-bis(tetrazol-1-yl)-2-methylpropane (btzmp),¹⁸ *m*-xylylenebis(tetrazole) (btzx)³⁴ only btzb forms 3D polymeric species whereas the others were isolated as 1D networks. Other homological ligands containing longer alkyl spacer (pentyl, heksyl ect.) form SCO complexes with Fe(II), but to our best knowledge particular crystal structures have not been determined yet.^{35,36} Among the above mentioned systems only $[\text{Fe}(\mu\text{-btzmp})_2(\text{btzmp})_2](\text{ClO}_4)_2$ and $[\text{Fe}(\text{btzb})_3](\text{PF}_6)_2 \cdot n\text{Solv}$ (*nSolv*: 0.075MeOH, 0.25EtOH) display abrupt spin transitions. Remaining complexes containing bis(tetrazol-1-yl)alkanes exhibit gradual SCO.

Received: July 19, 2011

Published: October 28, 2011

It is supposed that contrary to $[\text{Fe}(\mu\text{-btzmp})_2(\text{btzmp})_2]-(\text{ClO}_4)_2$, a weak cooperativity in $[\text{Fe}(\text{btzp})_3](\text{ClO}_4)_2$ and $[\text{Fe}(\text{endi})_3](\text{BF}_4)_2$ systems results from a flexibility of alkyl spacer (shock absorber effect) and low crystal packing.

Taking into account that also rigidity of a coordination network, resulting from its architecture, may decisively influence SCO properties,³⁷ we have decided to expand our investigations on an application of tripodal ligands in construction of SCO coordination polymers. Contrary to bis(azole)-type ligands, tridentate systems are potentially capable of binding three adjacent metal ions and give an opportunity to form networks with topologies not available using bidentate ligands. Properties of azole based tripodal ligands as building blocks strongly depend on the kind of donor group and the position of substituent in the ring. An application of tripodal ligands containing azole rings with an *endo* positioned nitrogen donor atom does not favor formation of coordination networks. They act rather as chelating systems giving molecular species.³⁸ An interesting feature of tripodal ligands containing pyrazol-1-yl and imidazol-2-yl³⁹ donors is an ability to form molecular cages. Ligand systems with imidazol-1-yl donors, that is, possessing *exo* located nitrogen donor atoms reacting with metal ions give molecular cages;⁴⁰ however, they are also prone to form coordination networks.⁴¹ Hence a choice of monodentate coordinating azole donor groups comprising *exo* located nitrogen atoms like tetrazol-1-yl, tetrazol-2-yl, or 1,2,3-triazol-1-yl are treated with priority in the endeavor to synthesize coordination polymers. A number of SCO complexes based on tripodal nonchelating azole-based ligands is very limited. Tris[2-(tetrazol-1-yl)ethyl]amine (entz) in a reaction with iron(II) tetrafluoroborate forms 2D coordination polymer showing abrupt spin transition.^{27,42} In spite of the presence of an apical nitrogen atom, entz acts as tridentate ligand, bridging three adjacent iron(II) ions through N4 atoms of tetrazole rings. Tris-3-[1,2,4]triazol-4-yl-propyl phloroglucinol (trptrz) is another example of tripodal ligand suitable for construction of SCO coordination networks.⁴³ Trptrz reacting with iron(II) tetrafluoroborate gives SCO compound of formula $[\text{Fe}(\text{trptrz})_2](\text{BF}_4)_2 \cdot 5\text{H}_2\text{O}$. Taking into account the above presented successful attempts to apply tripodal ligands for construction of SCO networks, we have synthesized a novel tridentate ligand 1,1',1''-tris(tetrazol-1-ylmethyl)methane (**111tz**) containing tetrazol-1-yl as donor group. In this paper we report on two novel 2D coordination polymers $[\text{Fe}(\mathbf{111tz})_2](\text{ClO}_4)_2$ and $[\text{Fe}(\mathbf{111tz})_2](\text{BF}_4)_2$ showing abrupt and complete spin transitions. The results of variable temperature magnetic susceptibility measurements (5–300 K) and single crystal X-ray diffraction studies for $[\text{Fe}(\mathbf{111tz})_2](\text{ClO}_4)_2$ (293, 230, 185, 155, 100 K) and $[\text{Fe}(\mathbf{111tz})_2](\text{BF}_4)_2$ (293, 225, 195, 190, 185, 100K) are presented and discussed.

EXPERIMENTAL SECTION

Elemental analyses for carbon, nitrogen, and hydrogen were performed on a Perkin-Elmer 240C analyzer. Infrared spectra were recorded with a Bruker 113v FTIR spectrometer in the range 400–4000 cm^{-1} as a KBr pellets. ^1H and ^{13}C spectra were recorded using a Bruker AMX 300 MHz and Bruker Avance 500 MHz spectrometers in a CD_3CN solution with internal TMS reference. Temperature measurements of the magnetic susceptibility were carried out with a Quantum Design SQUID magnetometer in the 5–300 K temperature range operating at 1 T for **1** and 0.5 T for **2**. Magnetic data were corrected for the diamagnetic contributions, which were estimated from Pascal's constants. $\text{Fe}(\text{ClO}_4)_2 \cdot 6\text{H}_2\text{O}$, $\text{Fe}(\text{BF}_4)_2 \cdot 6\text{H}_2\text{O}$, 3-chloro-2-(chloromethyl)prop-1-ene, and sodium were purchased from Aldrich;

diethyl azodicarboxylate was purchased from Fluka and used without further purification. Acetonitrile and methanol used for chromatography were HPLC grade. Dichloromethane was distilled before use. Acetonitrile for syntheses was dried by a distillation over calcium hydride. Tetrazole was synthesized according to the known method.⁴⁴ The complexes were synthesized under nitrogen atmosphere using standard Schlenk technique.

Caution! Even though no problems were encountered it is worth mentioning that complexes containing perchlorates as well as tetrazole ligands are potentially explosive and should be synthesized and handled with care.

Synthesis of 1-Bromo-3-chloro-2-(chloromethyl)propane.

1-Bromo-3-chloro-2-(chloromethyl)propane was obtained in the radical addition of hydrogen bromide to the 3-chloro-2-(chloromethyl)prop-1-ene. Dry hydrogen bromide was slowly passed through the mixture of 3-chloro-2-(chloromethyl)prop-1-ene (1.0 g; 0.008 mol) in pentane (200 mL). One drop of diethyl azodicarboxylate (DEAD) was used to initiate the radical reaction. The mixture was stirred for 2 h and irradiated by UV light (500 W lamp). The resulting colorless pentane solution was flushed with N_2 to remove most of the HBr and then washed repeatedly with saturated aqueous Na_2CO_3 solution. The resulting organic solution was then dried (Na_2SO_4) and concentrated under reduced pressure. The obtained colorless oil was used without further purification. Yield 1.56 g (95%), ^1H NMR CD_3CN , $\delta = 3.75$ (d, 4H); 3.62 (d, 2H); 2.45 (m, 1H) ppm; ^{13}C NMR CD_3CN , $\delta = 45.43$; 44.80; 32.87 ppm.

IR (film on KBr): ν cm^{-1} : 2960 (s) 2858 (vw), 1438 (vs), 1379 (vw), 1344 (w), 1325 (s), 1274 (s), 1203 (w), 1080 (vw), 1053 (vw), 971 (vw), 894 (m), 853 (s), 822 (s), 748 (s), 698 (s), 655 (w), 633 (m), 606 (vw), 517 (vw), 482 (vw), 408 (vw).

Synthesis of 1-[3-Chloro-2-(chloromethyl)propyl]-1H-tetrazole (1tzCl2). Into dehydrated methanol (50 mL) was added sodium (2.3 g; 0.1 mol). After completion of the reaction, tetrazole (7.0 g; 0.1 mol) was added. Then methanol was removed under reduced pressure. The obtained sodium tetrazolate was suspended in acetonitrile (200 mL), and 1-bromo-3-chloro-2-(chloromethyl)propane (20.0 g; 0.097 mol) was added. The reaction mixture was stirred and refluxed for 3 days. After cooling, the precipitate of NaBr was filtered off and solvents were evaporated under reduced pressure. The obtained pale yellow oil (20.5 g) was purified by column chromatography on silica gel (230 mesh) using CH_2Cl_2 as eluent ($R_f = 0.40$). Yield 5.95 g (31.2%), ^1H NMR CDCl_3 , $\delta = 8.73$ (s, 1H); 4.67 (d, 2H); 3.50–3.75 (m, 4H); 2.84 (m, 1H) ppm; ^{13}C NMR CD_3CN , $\delta = 145.12$; 47.87; 43.90; 43.71 ppm. IR (film on KBr); ν cm^{-1} : 3137 (s), 3009 (w), 2963 (w), 1483 (s), 1442 (vs), 1301 (m), 1284 (s), 1171 (vs), 1103 (vs), 1026 (m), 963 (m), 875 (m), 832 (w), 660 (s), 519 (vw).

Synthesis of Tris(tetrazol-1-ylmethyl)methane (111tz). Sodium tetrazolate was obtained as described for 1tzCl2 using sodium (3.54 g, 0.154 mol), tetrazole (10.78 g, 0.154 mol), and methanol (60 mL). To the suspended sodium tetrazolate in acetonitrile (250 mL) was added 1-[3-chloro-2-(chloromethyl)propyl]-1H-tetrazole (10.92 g, 0.056 mol) dissolved in acetonitrile (20 mL). The reaction mixture was stirred and refluxed for 14 days. After cooling, the precipitate of NaCl was filtered off, and solvents were evaporated under reduced pressure. The obtained pale yellow oil (11.4 g) was purified by column chromatography on silica gel (230–400 mesh). An elution was performed using the following eluents: $\text{CH}_2\text{Cl}_2/\text{MeCN}/\text{MeOH}$ 10/1.0/0.4 (v/v), $\text{CH}_2\text{Cl}_2/\text{MeCN}/\text{MeOH}$ 10/1.0/0.8 (v/v), $\text{CH}_2\text{Cl}_2/\text{MeCN}/\text{MeOH}$ 10/1.0/1.2 (v/v) and three fractions containing **111tz**, 1-(tetrazol-1-ylmethyl)-1',1''-di(tetrazol-2-ylmethyl)methane (**221tz**) and 1,1'-di(tetrazol-1-ylmethyl)-1''-(tetrazol-2-ylmethyl)methane (**211tz**) were collected.

111tz Yield: 1.15 g (7.8%) *Anal.* Found C%, 32.1; N%, 64.1; H%, 3.7; Calc. for $\text{C}_7\text{N}_{12}\text{H}_{10}$ C%, 32.1; N%, 64.1; H%, 3.8; ^1H NMR CD_3CN , $\delta = 8.92$ (s, 3H); 4.53 (d, 6H); 3.30–3.40 (m, 1H) ppm; ^{13}C NMR CD_3CN , $\delta = 145.99$; 48.06; 41.10 ppm. IR (KBr): ν cm^{-1} : 3148 (w), 3127 (m), 3088 (vs), 2989 (m), 2954 (w), 2921 (w), 1484 (vs), 1444 (s), 1433 (s), 1376 (w), 1259 (m), 1187 (vs), 1135 (m), 1115 (vs), 1097 (vs), 1025 (m), 977 (s), 903 (w), 887 (w), 835 (vw), 798 (vw), 782 (vw), 750 (vw), 739 (vw), 717 (w), 705 (w), 661 (m),

Table 1. Crystallographic Data for **1**, **2**, and **111tz**

	1						111tz
formula	FeCl ₂ O ₈ C ₁₄ N ₂₄ H ₂₀						C ₇ N ₁₂ H ₁₀
M _w	779.22						262.24
T (K)	293(2)	230(2)	185(2)	155(2)	100(2)	230(2)	100(2)
λ (Å)	0.71073						
space group	P $\bar{3}$						Pc
a (Å)	10.064(3)	10.057(3)	10.022(3)	9.917(3)	9.891(2)	10.048(3)	14.545(3)
b (Å)							6.432(2)
c (Å)	8.454(3)	8.446(4)	8.429(2)	8.372(2)	8.352(3)	8.444(2)	11.973(2)
β (deg)							93.11(2)
V (Å ³)	741.5(4)	739.8(5)	733.2(4)	713.0(3)	707.6(3)	738.3(4)	1118.5(1)
Z	1						4
D _c (Mg·m ⁻³)	1.745	1.749	1.765	1.815	1.829	1.753	1.557
μ (mm ⁻¹)	0.775	0.777	0.784	0.806	0.813	0.779	0.115
R _I (I > 2σ _I)	0.035	0.031	0.034	0.028	0.029	0.036	0.034
wR ² (I > 2σ _I)	0.072	0.072	0.072	0.066	0.068	0.079	0.079
	2						
formula	FeB ₂ F ₈ C ₁₄ N ₂₄ H ₂₀						
M _w	753.93						
T (K)	293(2)	225(2)	195(2)	190(2)	185(2)	100(2)	225(2)
λ (Å)	0.71073						
space group	P $\bar{3}$						
a (Å)	10.159(3)	10.140(2)	10.115(3)	9.982(3)	9.967(3)	9.944(3)	10.146(3)
c (Å)	8.247(2)	8.222(4)	8.202(3)	8.161(2)	8.148(2)	8.126(2)	8.230(2)
V (Å ³)	737.1(4)	732.1(4)	726.7(4)	704.2(3)	701.0(3)	695.9(3)	733.7(3)
Z	1						
D _c (Mg·m ⁻³)	1.699	1.710	1.723	1.778	1.786	1.799	1.707
μ (mm ⁻¹)	0.619	0.623	0.627	0.647	0.650	0.655	0.621
R _I (I > 2σ _I)	0.032	0.037	0.034	0.037	0.032	0.031	0.030
wR ² (I > 2σ _I)	0.075	0.079	0.072	0.080	0.062	0.063	0.066

542 (vw), 520 (vw), 452 (vw). R_f = 0.11 [CH₂Cl₂/MeCN/MeOH 10/1.0/0.4 (v/v)].

221tz Yield: 1.74 g (11.8%). Anal. Found C%, 32.1; N%, 64.0; H%, 3.8; Calc. for C₇N₁₂H₁₀ C%, 32.1; N%, 64.1; H%, 3.8. ¹HNMR CD₃CN, δ = 8.88 (s, 1H); 8.63 (s, 2H); 4.80 (d, 4H); 4.56 (d, 2H); 3.58 (m, 1H) ppm; ¹³CNMR CD₃CN, δ = 153.88; 144.98; 51.99; 47.26; 39.43 ppm. IR (KBr): ν cm⁻¹: 3144 (s), 3132 (vs), 3004 (m), 2992 (w), 2964 (w), 2927 (vw), 1487 (w), 1454 (vs), 1430 (m), 1360 (m), 1287 (vs), 1254 (w), 1202 (m), 1190 (m), 1176 (s), 1141 (m), 1096 (vs), 1062 (w), 1040 (s), 1026 (s), 1016 (s), 968 (s), 918 (vw), 899 (m), 886 (w), 841 (vw), 807 (w), 764 (vw), 704 (s), 678 (m), 660 (s), 544 (vw), 521 (w), 511 (vw), 451 (vw). R_f = 0.55 [CH₂Cl₂/MeCN/MeOH 10/1.0/0.4 (v/v)].

211tz Yield: 2.05 g (13.9%). Anal. Found C%, 32.1; N%, 64.0; H%, 3.8; Calc. for C₇N₁₂H₁₀ C%, 32.1; N%, 64.3; H%, 3.7; ¹HNMR CD₃CN, δ = 8.90 (s, 2H); 8.65 (s, 1H); 4.75 (d, 2H); 4.54 (d, 4H); 3.46 (m, 1H) ppm; ¹³CNMR CD₃CN, δ = 153.32; 144.38; 51.13; 46.55; 39.15 ppm. IR (KBr): ν cm⁻¹: 3140 (s), 3095 (s), 2995 (m), 2966 (w), 2928 (vw), 1485 (s), 1459 (s), 1444 (s), 1395 (w), 1375 (m), 1348 (w), 1287 (s), 1254 (w), 1187 (vs), 1135 (s), 1098 (vs), 1070 (w), 1060 (w), 1027 (s), 970 (s), 917 (w), 897 (m), 834 (vw), 800 (vw), 782 (vw), 748 (w), 721 (w), 705 (m), 679 (m), 661 (s), 545 (vw), 523 (vw), 510 (vw), 451 (vw). Eluents: R_f = 0.22 [CH₂Cl₂/MeCN/MeOH 10/1.0/0.4 (v/v)].

Synthesis of the [Fe(111tz)₂](ClO₄)₂ (1**).** A solution of Fe-(ClO₄)₂·6H₂O (120 mg, 0.33 mmol) in 5 mL of deoxidized water was added to a warm solution of **111tz** (31.6 mg, 0.12 mmol) in 5 mL of deoxidized water (heated previously for ligand dissolving). The reaction mixture was heated up to 60 °C, and after cooling to room temperature a clear solution was left in a closed Schlenk flask. After 3 days, the colorless crystals of the complex were filtered off, washed by deoxidized water, and dried in a stream of nitrogen. Yield: 33.8 mg (72.3%). Anal. Calc. for FeCl₂O₈C₁₄N₂₄H₂₀: C, 21.56; H, 2.60; N,

43.12. Found: C, 21.60; H, 2.29; N, 42.97%. IR (KBr): ν cm⁻¹: 3131 (m), 3016 (vw), 1635 (br, vw), 1507 (m), 1450 (s), 1375 (vw), 1337 (vw), 1311 (vw), 1298 (vw), 1267 (w), 1187 (s), 1109 (vs), 991 (m), 886 (m), 760 (w), 745 (w), 717 (w), 662 (s), 621 (s), 462 (w).

Synthesis of the [Fe(111tz)₂](BF₄)₂ (2**).** A solution of the Fe(BF₄)₂·6H₂O (480 mg, 1.42 mmol) in 10 mL of deoxidized water was added to **111tz** (41.9 mg, 0.15 mmol) in 6 mL of deoxidized water. The reaction mixture was heated up to 60 °C, and after cooling a clear solution was left in a closed Schlenk flask. After 8 days, the colorless crystals of the complex were filtered off, washed by deoxidized water, and dried in a stream of nitrogen. Yield: 43.0 mg (76.0%). Anal. Calc. for FeB₂F₈C₁₄N₂₄H₂₀: C, 22.37; H, 2.53; N, 44.52. Found: C, 22.37; H, 2.53; N, 44.53%. IR (KBr): ν cm⁻¹: 3139 (m), 3023 (vw), 1635 (br, vw), 1507 (m), 1451 (s), 1379 (vw), 1339 (w), 1312 (w), 1299 (w), 1268 (w), 1188 (s), 1109 (vs), 1048 (vs), 992 (s), 887 (m), 761 (vw), 745 (w), 717 (w), 662 (s), 517 (w), 463 (vw).

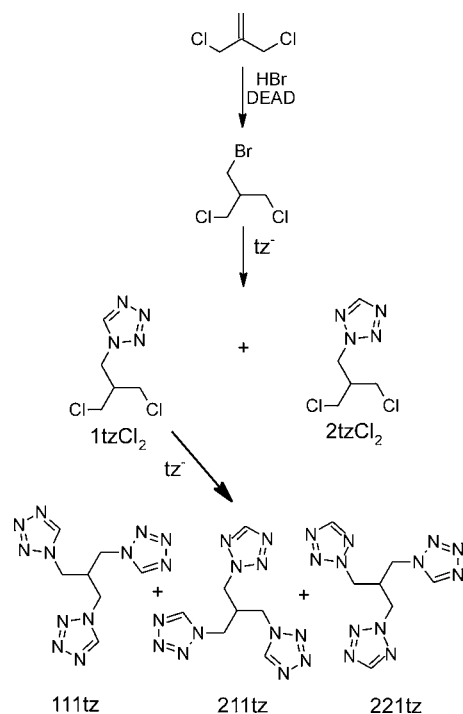
X-ray Data Collection and Structure Determination. The crystals of **1** and **2** suitable for X-ray measurements were selected from the crystalline product obtained according with aforementioned synthesis procedure of complexes. Crystals of **111tz** suitable for single crystal X-ray diffraction investigations were grown from acetonitrile solution. Crystals were coated by a layer of inert oil and immediately transferred to the stream of nitrogen of the diffractometer. Crystal data and refinement details for **1**, **2**, and **111tz** are listed in Table 1. All the measurements were performed using an Oxford Cryosystem device on Kuma KM4CCD κ-axis diffractometer with graphite-monochromated MoKα radiation. The data were corrected for Lorentz and polarization effects. Analytical absorption correction was applied for **1** and **2**. Data reduction and analysis were carried out with the Oxford Diffraction (Poland) Sp. z o.o. (formerly Kuma Diffraction Wrocław, Poland) programs. The structures were solved by direct methods (program

SHELXS97⁴⁵) and refined by the full-matrix least-squares method using all F^2 data, as implemented by the SHELXL97 program.

RESULTS AND DISCUSSION

Ligand Synthesis and Characterization. An alkylating agent, that is, 1-bromo-3-chloro-2-(chloromethyl)propane, was synthesized by radical addition of HBr to the 3-chloro-2-(chloromethyl)prop-1-ene in pentane solution (see Scheme 1).

Scheme 1



It is well-known that alkylation of tetrazole is not regioselective and leads to formation of comparable amounts of 1- and 2-substituted derivatives.⁴⁶ Therefore to avoid formation at the same time of all tris(tetrazole) derivatives, making isolation of desired products difficult, substitution of halides was carried out in two steps. In the first step, only one bromine atom was replaced by tetrazole resulting in 1tzCl₂ and 2tzCl₂. In the second step, reaction performed between isolated 1tzCl₂ and sodium tetrazolate gave three compounds: **111tz**, **211tz**, and **221tz**. **111tz** crystallizes as a colorless crystals soluble in cold water and is poorly soluble in acetonitrile, methanol, and acetone.

Crystal and Molecular Structure of the 111tz. The ligand crystallizes in the monoclinic system, the space group Pc (Table 1). A crystallographically unrelated part of the unit cell consists of two **111tz** molecules denoted as A and B possessing different conformations (Figure 1). The main difference between molecules A and B depends on different conformation of one of three arms. C3–C2–C1–N5 and C3A–C2A–C1A–N5A torsion angles are equal to $-176.19(1)^\circ$ and $61.68(2)^\circ$, respectively (Supporting Information, Figure S1). Packing of **111tz** molecules in the crystal is stabilized by presence of weak C–H...N intermolecular interactions (see Supporting Information, Table S1 and Figure S2)

Synthesis and General Characterization of [Fe(111tz)₂](ClO₄)₂ (1) and [Fe(111tz)₂](BF₄)₂ (2). The successful preparation of complexes were performed in water

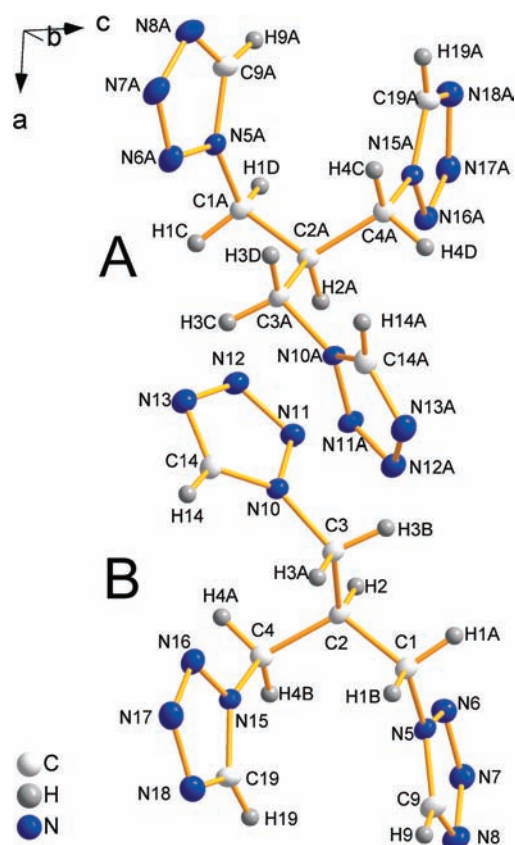


Figure 1. Molecular structure of the **111tz** in the solid state (50% ellipsoids) together with labeling scheme of atoms.

solution applying a significant excess of appropriate Fe(II) salt in relation to **111tz** amounts. Attempts of **1** and **2** synthesis carried out with stoichiometry Fe(II)/**111tz** 1:2 failed and crystallization of the ligand takes place. Increasing the Fe(BF₄)₂·6H₂O to **111tz** molar ratio to 12:1 involves crystallization of complex as well as unreacted ligand. It was found that only large excess of Fe(BF₄)₂·6H₂O, that is, about 19:1, leads to formation only one product [Fe(**111tz**)₂](BF₄)₂. For a change, successful preparation of **1** occurs when the molar ratio of Fe(ClO₄)₂·6H₂O to **111tz** is equal to 6:1. Although syntheses of **1** and **2** were performed with large excess of iron(II) salts, the product compositions are the same, that is, [Fe(**111tz**)₂](ClO₄)₂ (X = ClO₄⁻, BF₄⁻). Both complexes have grown as colorless crystals that were stable during storage under nitrogen atmosphere.

Preliminary investigations showed that cooling of the crystal samples of **1** and **2** in liquid nitrogen is accompanied with a change in color from white to purple. This behavior indicates HS→LS transitions in both complexes.

Magnetic Studies of [Fe(111tz)₂](ClO₄)₂ (1) and [Fe(111tz)₂](BF₄)₂ (2). Magnetic data for compounds **1** and **2** have been recorded in the temperature range 5–300 K. The χ_{MT} vs T (χ_{MT} , molar susceptibility; T , temperature) are shown in Figure 2. In the temperature range from 300 to 210 K the value of χ_{MT} for **1** is almost constant and is equal to 3.65 cm³ K/mol. In this temperature threshold the χ_{MT} value for **2** is equal to 3.40 cm³ K/mol. These χ_{MT} values are characteristic for the HS form of Fe(II) ion. Further lowering of temperature involves in both complexes a very abrupt HS→LS transition with $T_{1/2}^{\downarrow} = 176$ K for **1** and 192.8 K for **2**. In the heating mode the course of the $\chi_{MT}(T)$ dependency in **1** is the same as that

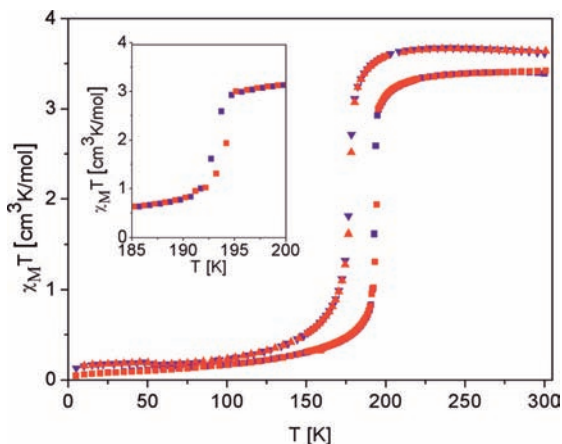


Figure 2. $\chi_M T$ vs T plots for **1** (triangles) and **2** (squares) in cooling (blue) and heating (red) modes.

observed in the cooling cycle. The spin transition in **2** is accompanied by a very narrow hysteresis loop of width of about 1 K ($T_{1/2}^\uparrow = 193.8$, $T_{1/2}^\downarrow = 192.8$ K).

X-ray Diffraction Studies of 1 and 2. Crystal structures at 293, 230*, 185, 155, and 100 K for **1** and at 293, 225*, 195, 190, 185, and 100 K for **2** were determined in cooling mode (*, measurements performed in a heating mode). Both complexes are isostructural and crystallize in the $P\bar{3}$ space group, in the trigonal crystal system (Table 1). An asymmetric part of the unit cell consists of iron(II) ion, part of **111tz** molecule, and disordered anion (Figure 3). Iron(II) ion, apical carbon atom of **111tz** molecule, and chlorine atom of perchlorate anion for **1** or boron atom of tetrafluoroborate anion for **2** are located in the special positions. The first coordination sphere of Fe(II) ions in **1** and **2** is composed of six tetrazole rings. The tetrazole moieties coordinate monodentately to the Fe(II) ion through the N4 nitrogen atom and form a slightly distorted octahedron. In **1** the N4–Fe–N4(y , $-x+y$, $-z$) and N4–Fe–N4($-y$, $x-y$, z) angles adopt values of $91.38(7)^\circ$ and $88.62(7)^\circ$ at 293 K and $91.17(5)^\circ$ and $88.83(5)^\circ$ at 100 K, respectively. In **2** suitable angles are closer to 90° and are equal to $91.01(5)^\circ$ and $88.99(5)^\circ$ at 293 K and $90.86(6)^\circ$ and $89.14(6)^\circ$ at 100 K.

At 293 and 230 K, the Fe–N4 distance in **1** is equal to 2.171(2) and 2.172(2) Å, respectively, which is in the range expected for the HS form of iron(II) ion. At 185 K, a slight decrease of the iron–nitrogen distance to 2.151(2) Å takes place. An observed shortening of the Fe–N distance is due to occupation of the crystallographically equivalent sites by HS and LS iron(II) ions. The spin fraction depends linearly on an average shortening of metal–ligand distance and may be estimated from the equation $\gamma_{\text{HS}} = (d_T - d_{\text{LS}})/(d_{\text{HS}} - d_{\text{LS}})$ (where γ_{HS} is the HS molar fraction at temperature T ; d_{HS} , d_{LS} , d_T are the Fe–N distances for HS, LS, and observed at temperature T forms, respectively).⁴⁷ Thus, the observed shortening of the Fe–N distance at 0.02 Å indicates a presence in the crystal lattice of about 10% of Fe(II) ions in the LS state at 185 K (see Supporting Information, Figure S3). Further lowering of temperature induces an abrupt HS→LS transition and at 155 K the Fe–N distance equals 2.021(1) Å. The change of metal–ligand bond length corresponds to the presence of about 10% iron(II) ions remaining in the HS form. At 100 K the Fe–N distance is equal to 2.002(1) Å.

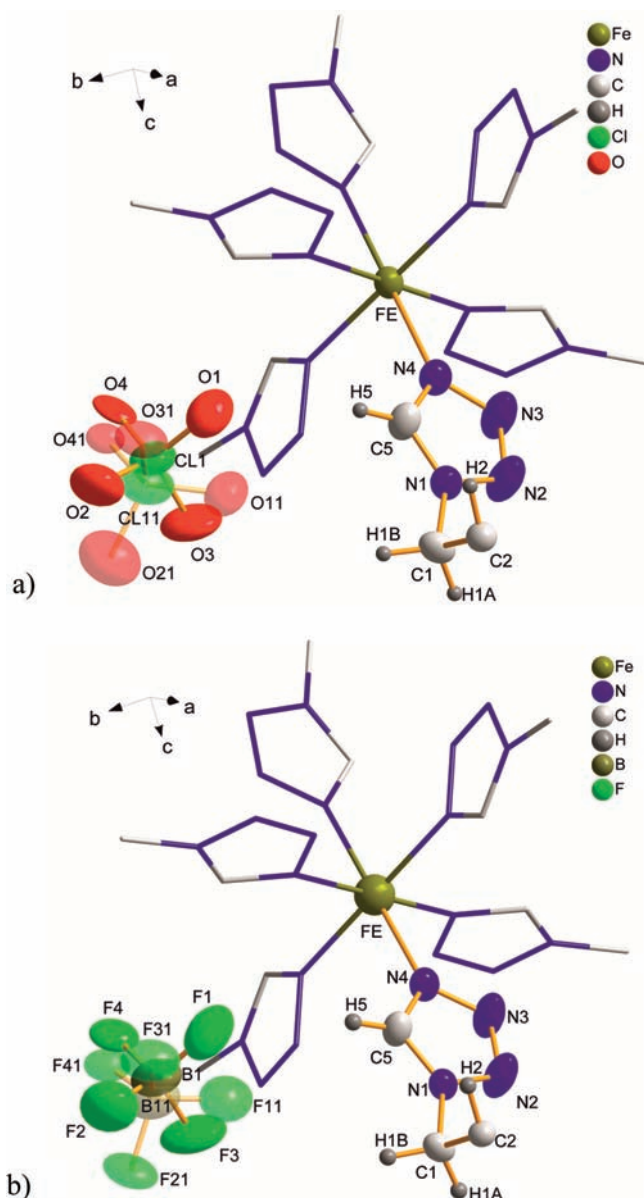


Figure 3. Asymmetric part of the unit cell (50% ellipsoids) and coordination environment of Fe(II) in $[\text{Fe}(\mathbf{111tz})_2](\text{ClO}_4)_2$ **1** (a) and $[\text{Fe}(\mathbf{111tz})_2](\text{BF}_4)_2$ **2** (b). Transparency was used for the minor component of disordered anions.

In **2**, at 293 K the Fe–N4 distance is equal to 2.179(2) Å. Temperature lowering involves a slight reduction of the metal–ligand distance to 2.169(2) at 225 K ($\gamma_{\text{HS}} \approx 0.95$) and 2.152(2) at 195 K ($\gamma_{\text{HS}} \approx 0.86$). A temperature drop to 190 K leads to an abrupt decrease of the Fe–N distance to a value of 2.015(1) Å. Below 190 K a slight shortening occurs of the Fe–N distance to 2.004 Å at 185 K ($\gamma_{\text{HS}} \approx 0.18$) and to 1.987(2) Å at 100 K. The observed alterations of Fe–N distances in **1** and **2** correspond to results of magnetic studies.

The tridentate **111tz** ligand molecules act as a μ_3 bridging unit joining three neighboring Fe(II) ions (Figure 4a). In turn, two neighboring Fe(II) ions are linked to each other by two ligand molecules which form double bridges. One Fe(II) ion is linked to six neighboring Fe(II) ions by the double bridges, along the [100], [010], [−100], [0−10], [110], and [−1−10] directions, resulting in formation of a 2D polymeric layer with a

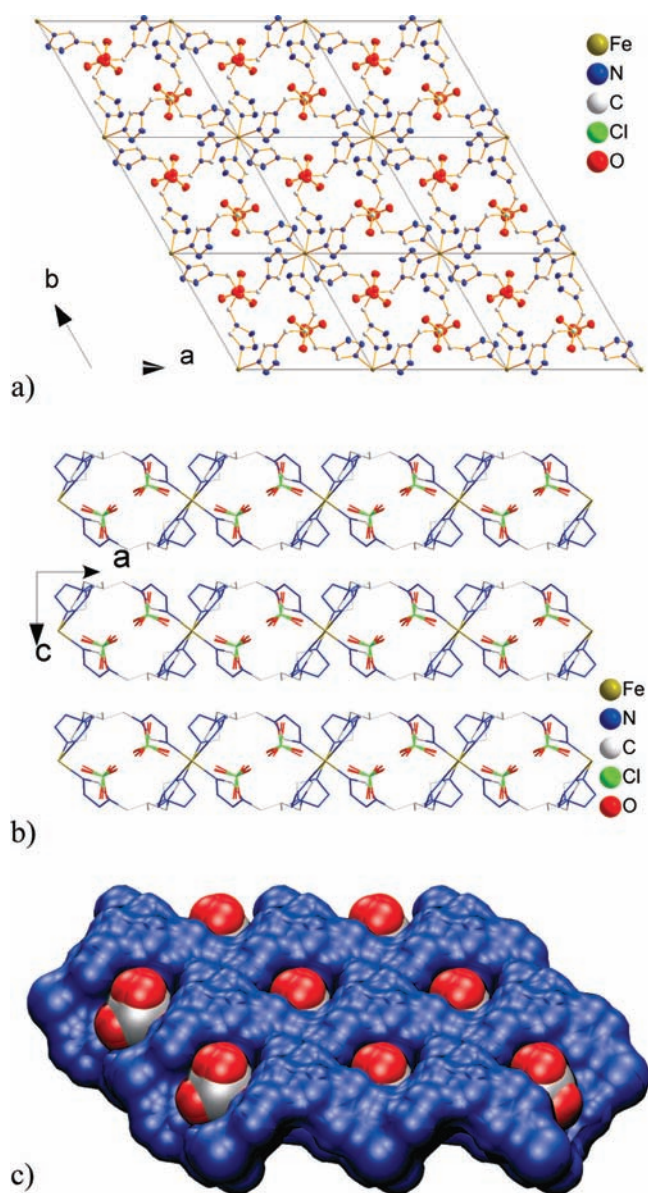


Figure 4. View of a single layer (a), a packing of 2D layers (b), and anions occupying cages in the 2D layer (c) in $[\text{Fe}(\mathbf{111tz})_2](\text{ClO}_4)_2$.

honeycomb-type grid (Figure 4a–c). An application of tris[2-(tetrazol-1-yl)ethyl]amine,^{42,48} 1,3,5-tris(imidazol-1-yl)benzene,^{41d} or 1,3,5-tris(imidazol-1-yl)-2,4,6-trimethylbenzene^{41b,c,e} ligands in coordination polymer syntheses afforded in the formation of networks with the same topology. Also in these complexes metal ions are homoleptically surrounded by six azole rings. In **1** at 293 K the distance between the bridged iron(II) ions is equal to 10.064(3) Å. Lowering the temperature from 293 to 185 K leads to a decrease of the intralayer Fe...Fe distance to 10.022(3) Å. The HS→LS transition causes abrupt shortening of the distance between the bridged Fe(II) ions to 9.917(3) Å. At 100 K the bridged iron(II) ions are separated at distances of 9.891(2) Å. In the tetrafluoroborate analogue the distance between joined iron(II) ions at 293 K is about 0.1 Å more distant than the ones found in **1** (see Table 2). Similarly to **1** temperature decrease involves initially a slight reduction of the intralayer Fe...Fe separation in **2** from 10.159(3) Å at 293 K to 10.115(3) Å at 195 K and further temperature lowering is accompanied by abrupt reduction of the Fe...Fe separation to

9.967(3) Å at 185 K. At 100 K the iron(II) ions are separated at a distance of 9.944(3) Å.

In **1**, the shortest interlayer Fe...Fe separation (along *c*) at 293 K is equal to 8.454(3) Å. The shortest Fe...Fe distance between iron(II) ions from adjusted layers decreases during temperature lowering. At 185 K the Fe...Fe distance is equal to 8.429(2) Å. Between 185 and 155 K a more abrupt reduction of interlayer separation takes place at about 0.06 Å. At 100 K the Fe...Fe distance is equal to 8.352(3) Å. In **2** at 293 K, the shortest interlayer Fe...Fe separation (along *c* direction) equals 8.247(2) Å, and this distance is shorter at about 0.2 Å in relation to the interlayer Fe...Fe distance in **1**. Temperature dependence of the Fe...Fe separation in **2** is similar to the one observed for the perchlorate analogue. More abrupt reduction of the interlayer separation in **2** (at about 0.05 Å) occurs during HS→LS transition, and the interlayer Fe...Fe distance after the spin transition remains about 0.2 Å shorter than in **1**. During temperature decrease, also a layer thickness (measured as a distance between planes defined by suitable apical carbon atoms) undergoes reduction, and the difference in the layer thickness between 273 and 100 K is equal to 0.32 Å.

The cationic layers abound in cavities with the apical C2 atom at their bottom. The cavities are occupied by ClO_4^- or BF_4^- anions in **1** and **2**, respectively (Figure 4c). The perchlorate and tetrafluoroborate anions reveal a huge degree of disorder (Supporting Information, Figure S4).

In the assumed model both chlorine and oxygen atoms in **1** or boron and fluorine atoms in **2** are disordered. Partially, chlorine (Cl1) in **1** or boron (B1) atom in **2** of the disordered anions are located in a special position (3-fold axis). In other parts of the disordered anions, chlorine (Cl11) or boron (B11) atoms are found close to the special position. In **1** at 293 K the occupancy factor of perchlorate anions with chlorine atom located in the special position is equal to 0.78, and the factor increases with lowering of temperature from 0.84 at 230 K, 0.89 at 185 K, and 0.83 in 155 K. At 100 K perchlorate anions are still disordered and anions with chlorine atom placed in the general position comprise about 7%. In **2** the occupancy factor of anions with boron atom located in the special position reaches values of 0.75 at 293 K, 0.82 at 225 K, 0.85 at 195 K, 0.87 at 190 K, and 0.86 at 185 K. Both decrease of interlayer separation and layer's thickness reduction are associated with shortening of distance between anion and apical carbon atom C2. It is worth emphasizing that in both complexes the HS→LS transition does not lead to vanishing of anion disorder in **1**. However, in **2** anion disorder disappears at 100 K. The cause of the observed disorder is a large size of voids in relation to anion volume. Volumes accessible for anions in **1** and **2** are equal to about 89 and 86 Å³, at 230 and 225 K, respectively.⁴⁹ These volumes are about two times higher than calculated molecular volumes for perchlorate and tetrafluoroborate anions.⁵⁰ At 100 K these volumes are reduced to 77 and 75 Å³, respectively. For comparison, in the HS phase (130 K) of another 2D coordination polymer $[\text{Fe}(\text{bbtr})_3](\text{ClO}_4)_2$ the volume occupied by ordered perchlorate anion is equal to about 62 Å³.^{31b}

Anions are engaged in formation of C–H...O(ClO_4^-) or C–H...F(BF_4^-) weak intermolecular interactions (see Supporting Information, Figure S4). In both complexes anions are disordered in very similar manner. Also networks of intermolecular interactions in both complexes are comparable (see Supporting Information, Table S3 for details).

The shortest distance between Fe(II) and Cl1(ClO_4^-)(1–*y*, *x*–*y*, *z*) at temperature of 293 K is equal to 5.887(1) Å, and it

Table 2. Selected Fe–N Distances (Å), N4–Fe–N4 Angles (deg), Σ^a , N4–N4A and Fe–X (X = Cl or B) Interatomic Distances (Å) for **1** at 293, 230, 185, 155, and 100 K and **2** at 293, 225, 195, 190, 185, and 100 K

		1					
temp	293 K	230 K	185 K	155 K	100 K	230 K ^(*)	
Fe–N	2.171(2)	2.172(2)	2.151(2)	2.021(1)	2.002(1)	2.169(2)	
N4–Fe–N4 ⁽¹⁾	91.38(7)	91.40(7)	91.24(7)	91.19(6)	91.17(5)	91.31(7)	
N4–Fe–N4 ⁽²⁾	88.62(7)	88.60(7)	88.76(7)	88.81(6)	88.83(5)	88.69(7)	
Σ	16.56	16.80	14.88	14.28	14.04	15.72	
N4–N4 ⁽³⁾	7.076(2)	7.071(2)	7.063(2)	7.138(2)	7.138(1)	7.063(2)	
Fe–1X	5.887(1)	5.881(1)	5.859(1)	5.812(1)	5.796(1)	5.876(1)	
Fe–11X ⁽⁴⁾	5.650(2)	5.582(2)	5.553(2)	5.508(2)	5.331(1)	5.573(2)	
C5–N1–C1–C2	–93.06	–93.04	–93.11	–94.48	–94.73	–92.69	
N1–C1–C2–C1 ⁽³⁾	–69.27	–69.39	–68.88	–68.43	–67.95	–69.45	
		2					
temp	293 K	225 K	195 K	190 K	185 K	100 K	225 K ^(*)
Fe–N	2.179(2)	2.169(2)	2.152(2)	2.015(1)	2.004(1)	1.987(2)	2.174(1)
N4–Fe–N4 ⁽²⁾	88.99(6)	89.08(7)	89.21(6)	89.10(4)	89.10(6)	89.14(6)	89.12(6)
N4–Fe–N4 ⁽¹⁾	91.01(6)	90.92(7)	90.79(6)	90.90(4)	90.90(6)	90.86(6)	90.88(6)
Σ	12.12	11.04	9.48	10.08	10.08	10.32	10.56
N4–N4 ⁽³⁾	7.138(2)	7.130(1)	7.127(2)	7.190(2)	7.191(2)	7.192(2)	7.129(2)
Fe–1X	5.930(1)	5.916(1)	5.900(1)	5.836(1)	5.828(1)	5.813(1)	5.919(1)
Fe–11X ⁽⁴⁾	5.724(1)	5.694(1)	5.679(1)	5.570(1)	5.574(1)		5.694(1)
C5–N1–C1–C2	–95.25	–95.04	–96.15	–96.66	–96.41	–96.41	–95.32
N1–C1–C2–C1 ⁽³⁾	–69.94	–69.72	–69.39	–68.43	–68.81	–68.45	–69.55

^(*)Heating mode, numbers are indicating symmetry related atoms 1: $y, -x+y, -z$; 2: $-y, x-y, z$; 3: $1-y, x-y, z$; 4: $-x+y, 1-x, -z$; a: $\Sigma = [12/(90 - N4-Fe-N4)]$.

changes during the spin transition to 5.796(1) Å at 100 K. In the second compounds the distance Fe...B1(BF₄⁻)(1- $y, x-y, z$) are equal to 5.930(1) Å at 293 K and 5.813(2) Å at 100 K. For anions occupying the second alternative position the shortest distance between Fe(II) and Cl11(ClO₄⁻)(1- $y, x-y, z$) at temperature of 293 K is equal to 5.650(2) Å, and it changes during the spin transition to 5.331(1) Å at 100 K. In **2** the Fe...B11(BF₄⁻)(1- $y, x-y, z$) distance is equal to 5.724(2) Å at 293 K and 5.828(1) Å at 185 K (Table 2).

Generally, tetrazole based iron(II) SCO complexes comprising tetrafluoroborate anions exhibit slightly higher $T_{1/2}$ values in relation to the perchlorate analogues. It is supposed that the iron-anion distance should correlate with the degree of coordination figure distortion (Σ), thus influencing the temperature of a spin transition.³¹ This general trend is also visible for complexes **1** and **2**. [Fe(**111tz**)₂](BF₄)₂ showing HS→LS transition at 193 K possess a slightly more regular chromophore FeN₆ ($\Sigma = 12.1^\circ$ at 293 K) in comparison with [Fe(**111tz**)₂](ClO₄)₂ ($\Sigma = 16.6^\circ$ at 293 K) which exhibits a spin transition at 176 K. It is also worth noticing that iron to anion distances in **1** and **2**, longer than the one observed for polymeric systems based on bis(tetrazole) ligands, correspond to higher $T_{1/2}$ values.

CONCLUDING REMARKS

Novel tripodal ligands containing tetrazole rings as donor groups were prepared. In this paper we have also presented products of reactions performed between tris(tetrazol-1-ylmethyl)methane (**111tz**) and perchlorate as well as tetrafluoroborate iron(II) salts. Complexes [Fe(**111tz**)₂](ClO₄)₂ (**1**) and [Fe(**111tz**)₂](BF₄)₂ (**2**) are isomorphous and were isolated as 2D coordination polymers. In accordance with our expectations **111tz** molecule serves as three-connecting ligand coordinating through N4 nitrogen atoms of the tetrazole rings. In both complexes ligand molecules bridge

iron(II) ions gathered in the common plane which leads to formation of 2D layers with honeycomb-like pattern. Spider-like shaped coordinated **111tz** molecules form cavities occupied by anions. The characteristic feature of the architecture of both complexes is the misfit between size of the cavities in 2D layers and anions' size. The size of these pockets is greater than demanded for the anions fitting. In effect anions are severely disordered adopting few positions and orientations. Counterions are engaged in formation of weak intermolecular interactions with hydrogen atoms of the same layer as well as with hydrogen atoms from the neighboring layer. Thus 2D polymeric units are tethered through a system of intermolecular interactions into a 3D supramolecular structure.

Complexes **1** and **2** show abrupt and complete spin transitions with $T_{1/2}^\uparrow = T_{1/2}^\downarrow = 176$ K and $T_{1/2}^\uparrow = 193.8$ and $T_{1/2}^\downarrow = 192.8$ K, respectively, accompanied by a thermochromic effect. In both compounds Fe–N4 bond lengths at 293 K are characteristic for HS iron(II) ions and lie in the range comparable to iron(II) complexes with 1-substituted tetrazoles. In **1** and **2**, the HS→LS transition is accompanied by shortening of the Fe–N distance at 0.17 and 0.19 Å, respectively. Spin transitions involve, in both complexes, reductions of iron...iron intralayer separations at about 0.11 Å. Shortening of the Fe–N distances also trigger a shift of **111tz** molecules toward the polymeric layer at about 0.14 Å. It results in shortening of distances between iron(II) ions from adjusted 2D polymeric units. In spite of the reduction of layer thickness, its corrugated nature after HS→LS transition causes that anions remain within the layer boundary, and they are still disordered. Negligible effect of spin transition on anion is observed. On the other hand different critical temperatures prove that kind of anion influence on SCO properties of this family of 2D polymeric systems.

The results presented here are encouragement for the continuation of further investigations of this ligand family

especially taking into account interesting relations between fitting of other anions into coordination network structure and SCO properties.

■ ASSOCIATED CONTENT

● Supporting Information

Crystallographic information files (CIFs) for **111tz**, **1** and **2**. Tables S1, S2 and S3 containing intermolecular contacts in **111tz**, **1** and **2**, respectively, and Figures S1, S2, S3, and S4. This material is available free of charge via the Internet at <http://pubs.acs.org>.

■ AUTHOR INFORMATION

Corresponding Author

*E-mail: robert.bronisz@chem.uni.wroc.pl (R.B.), marek.weselski@chem.uni.wroc.pl (M.W.).

■ ACKNOWLEDGMENTS

We thank the Ministry of Science and Higher Education for their financial support of this research (Grant 2493/B/H03/2008/34).

■ REFERENCES

- Gütlich, P.; Hauser, A.; Spiering, H. *Angew. Chem., Int. Ed. Engl.* **1994**, *33*, 2024–2054.
- Decurtins, S.; Gütlich, P.; Köhler, C. P.; Spiering, H.; Hauser, A. *Chem. Phys. Lett.* **1984**, *105*, 1–4.
- Decurtins, S.; Gütlich, P.; Hasselbach, K. M.; Spiering, H.; Hauser, A. *Inorg. Chem.* **1985**, *24*, 2174–2187.
- Gütlich, P.; Gaspar, A. B.; Ksenofontov, V.; Garcia, Y. *J. Phys.: Condens. Matter* **2004**, *16*, S1087–S1108.
- Kusz, J.; Spiering, H.; Gütlich, P. *J. Appl. Crystallogr.* **2001**, *34*, 229–238.
- Wiehl, L.; Spiering, H.; Gütlich, P.; Knorr, K. *J. Appl. Crystallogr.* **1990**, *23*, 151–160.
- Kitagawa, S.; Kitaura, R.; Noro, S. *Angew. Chem., Int. Ed.* **2004**, *43*, 2334–2375.
- Kahn, O.; Martinez, C. J. *Science* **1998**, *279*, 44–48.
- Guionneau, P.; Marchivie, M.; Bravic, G.; Leard, J.-F.; Casseau, D. *Top. Curr. Chem.* **2004**, *234*, 97–128.
- Spiering, H. *Top. Curr. Chem.* **2004**, *235*, 171–195.
- Halcrow, M. A. *Polyhedron* **2007**, *26*, 3523–3576.
- Real, J. A.; Gallois, B.; Granier, T.; Suez-Panama, F.; Zarembowitch, J. *Inorg. Chem.* **1992**, *31*, 4972–4797.
- Gallois, B.; Real, J. A.; Hauw, C.; Zarembowitch, J. *Inorg. Chem.* **1990**, *29*, 1152–1158.
- Zhong, Z. J.; Tao, J.; Yu, Z.; Dun, C.; Liu, Y.; You, X. *J. Chem. Soc., Dalton Trans.* **1998**, 327–328.
- van Koningsbruggen, P. J.; Garcia, Y.; Kooijman, H.; Spek, A. L.; Haasnoot, J. G.; Kahn, O.; Linares, J.; Codjovi, E.; Varret, F. *Dalton Trans.* **2001**, 466–471.
- Bartel, M.; Absmeier, A.; Jameson, G. N. L.; Werner, F.; Kato, K.; Takata, M.; Boca, R.; Hasegawa, M.; Mereiter, K.; Caneschi, A.; Linert, W. *Inorg. Chem.* **2007**, *46*, 4220–4229.
- Grunert, C. M.; Schweifer, J.; Weinberger, P.; Linert, W.; Mereiter, K.; Hilscher, G.; Muller, M.; Wiesinger, G.; van Koningsbruggen, P. J. *Inorg. Chem.* **2004**, *43*, 155–165.
- Quesada, M.; Kooijman, H.; Gamez, P.; Sanchez Costa, J.; van Koningsbruggen, P. J.; Weinberger, P.; Reissner, M.; Spek, A. L.; Haasnoot, J. G.; Reedijk, J. *Dalton Trans.* **2007**, 5434–5440.
- Schweifer, J.; Weinberger, P.; Mereiter, K.; Boca, M.; Reichl, C.; Wiesinger, G.; Hilscher, G.; van Koningsbruggen, P. J.; Kooijman, H.; Grunert, M.; Linert, W. *Inorg. Chim. Acta* **2002**, *339*, 297–306.
- van Koningsbruggen, P. J.; Garcia, Y.; Kahn, O.; Fournes, L.; Kooijman, H.; Spek, A. L.; Haasnoot, J. G.; Moscovici, J.; Provost, K.; Michalowicz, A.; Renz, F.; Gütlich, P. *Inorg. Chem.* **2000**, *39*, 1891–1900.
- (21) Vreugdenhil, W.; van Diemen, J. H.; de Graaff, R. A. G.; Haasnoot, J. G.; Reedijk, J.; van der Kraan, A. M.; Kahn, O.; Zarembowitch, J. *Polyhedron* **1990**, *9*, 2971–2979.
- (22) Real, J. A.; Andres, E.; Munoz, M. C.; Julve, M.; Granier, T.; Bousseksou, A.; Varret, F. *Science* **1995**, *268*, 265–267.
- (23) Moliner, N.; Munoz, C.; Letard, S.; Solans, X.; Menendez, N.; Goujon, A.; Varret, F.; Real, J. A. *Inorg. Chem.* **2000**, *39*, 5390–5393.
- (24) Halder, G. J.; Kepert, C. J.; Moubaraki, B.; Murray, K. S.; Cashion, J. D. *Science* **2002**, *298*, 1762–1765.
- (25) Kitazawa, T.; Gomi, Y.; Takahashi, M.; Takeda, M.; Enomoto, M.; Miyazaki, A.; Enoki, T. *J. Mater. Chem.* **1996**, *6*, 119–121.
- (26) (a) Niel, V.; Martinez-Agudo, J. M.; Munoz, C.; Gaspar, A.; Real, J. A. *Inorg. Chem.* **2001**, *40*, 3838–3839. (b) Munoz, M. C.; Real, J. A. *Coord. Chem. Rev.* **2011**, *255*, 2068–2093.
- (27) Garcia, Y.; Niel, V.; Munoz, C.; Real, J. A. *Top. Curr. Chem.* **2003**, *233*, 229–257.
- (28) Vreugdenhil, W.; Gorter, S.; Haasnoot, J. G.; Reedijk, J. *Polyhedron* **1985**, *4*, 1769–1775.
- (29) Ozarowski, A.; Shunzhong, Y.; McGarvey, B. R.; Mislankar, A.; Drake, J. E. *Inorg. Chem.* **1991**, *30*, 3167–3174.
- (30) Garcia, Y.; Kahn, O.; Rabardel, L.; Chansou, B.; Salmon, L.; Tuchagues, J. P. *Inorg. Chem.* **1999**, *38*, 4663–4670.
- (31) (a) Bronisz, R. *Inorg. Chem.* **2005**, *44*, 4463–4465. (b) Kusz, J.; Bronisz, R.; Zubko, M.; Bednarek, G. *Chem.—Eur. J.* **2011**, *17*, 6807–6820.
- (32) Aromí, G.; Barrios, A.; Roubeau, O.; Gamez, P. *Coord. Chem. Rev.* **2011**, *255*, 485–546.
- (33) (a) Galan-Mascaros, J. R.; Coronado, E.; Forment-Aliaga, A.; Monrabal-Capilla, M.; Pinilla-Cienfuegos, E.; Ceolin, M. *Inorg. Chem.* **2010**, *49*, 5706–5714. (b) Forestier, T.; Mornet, S.; Daro, N.; Nishihara, T.; Mouri, S.-I.; Tanaka, K.; Fouché, O.; Freysz, E.; Létard, J.-F. *Chem. Commun.* **2008**, 4327–4329. (c) Volatron, F.; Catala, L.; Riviere, E.; Gloter, A.; Stephan, O.; Mallah, T. *Inorg. Chem.* **2008**, *47*, 6584–6586.
- (34) Quesada, M.; Prins, F.; Bill, E.; Kooijman, H.; Gamez, P.; Roubeau, O.; Spek, A. L.; Haasnoot, J. G.; Reedijk, J. *Chem.—Eur. J.* **2008**, *14*, 8486–8499.
- (35) Absmeier, A.; Bartel, M.; Carbonera, C.; Jameson, G. N. L.; Werner, F.; Reissner, M.; Caneschi, A.; Létard, J. F.; Linert, W. *Eur. J. Inorg. Chem.* **2007**, 3047–3054.
- (36) Absmeier, A.; Bartel, M.; Carbonera, C.; Jameson, G. N. L.; Weinberger, P.; Caneschi, A.; Mereiter, K.; Letard, J.-F.; Linert, W. *Chem.—Eur. J.* **2006**, *12*, 2235–2243.
- (37) Enachescu, C.; Nishino, M.; Miyashita, S.; Hauser, A.; Stancu, A.; Stoleriu, L. *EPL* **2010**, *91*, 27003-p1–27003-p6.
- (38) Blackman, A. G. *Polyhedron* **2005**, *24*, 1–39.
- (39) (a) Su, C.-Y.; Cai, Y.-P.; Chen, C.-L.; Lissner, F.; Kang, B.-S.; Kaim, W. *Angew. Chem., Int. Ed.* **2002**, *41*, 3371–3375. (b) Hartshorn, C. M.; Steel, P. J. *Chem. Commun.* **1997**, 541. (c) Katsuki, I.; Matsumoto, N.; Kojima, M. *Inorg. Chem.* **2000**, *39*, 3350–3354. (d) Su, C.-Y.; Kang, B.-S.; Du, C.-X.; Yang, Q.-C.; Mak, T. C. W. *Inorg. Chem.* **2000**, *39*, 4843–4849.
- (40) Sun, W.-Y.; Fan, J.; Okamura, T.; Xie, J.; Yu, K.-B.; Ueyama, N. *Chem.—Eur. J.* **2001**, *7*, 2557–2562.
- (41) (a) Fan, J.; Sun, W.-Y.; Okamura, T.; Tang, W.-X.; Ueyama, N. *Inorg. Chem.* **2003**, *42*, 3168–3175. (b) Fan, J.; Sui, B.; Okamura, T.; Sun, W.-Y.; Tang, W.-X.; Ueyama, N. *J. Chem. Soc., Dalton Trans.* **2002**, 3868–3873. (c) Zhao, W.; Fan, J.; Okamura, T.; Sun, W.-Y.; Ueyama, N. *Microporous Mesoporous Mater.* **2005**, *78*, 265–279. (d) Lia, L.; Fan, J.; Okamura, T.; Li, Y.-Z.; Sun, W.-Y.; Ueyama, N. *Supramol. Chem.* **2004**, *16*, 361–370. (e) Yang, P.-P.; Ma, Z.-P.; Zhang, L.-Z.; Gu, W.; Liu, X. *Acta Crystallogr.* **2007**, *E63*, m233–m234.
- (42) (a) Bronisz, R.; Ciunik, Z.; Drabent, K.; Rudolf, M.; Uszyński, I. In *Condensed Matter Studies by Nuclear Methods*; E. A. Görlich., Tomala, K., Eds.; Jagiellonian University Press: Krakow, Poland, 1995; pp 372–377. (b) Bronisz, R.; Ciunik, Z.; Drabent, K.; Rudolf, M. In

Proceedings of the ICAME '95 Conference; Ortalli, I., Ed.; Italian Physical Society, 1996; Vol. 50, pp 15– 18.

(43) Boland, Y.; Hertsens, P.; Marchand-Brynaert, J.; Garcia, Y. *Synthesis* **2006**, 9, 1504–1512.

(44) (a) Kamiya, T.; Saito, Y. *Ger. Offen.* **1973**, 2147023. (b) Bronisz, R. *Inorg. Chim. Acta* **2002**, 340, 215–220.

(45) Sheldrick, G. M. *Acta Crystallogr., Sect. A* **2008**, 64, 112–122.

(46) (a) Begtrup, M.; Larsen, P. *Acta Chem. Scand.* **1990**, 44, 1050–1057. (b) Białońska, A.; Bronisz, R. *Tetrahedron* **2008**, 64, 9771–9779.

(47) Białońska, A.; Bronisz, R.; Darowska, K.; Drabent, K.; Kusz, J.; Siczek, M.; Weselski, M.; Zubko, M.; Ozarowski, A. *Inorg. Chem.* **2010**, 49, 11267–11269.

(48) (a) Werner, F.; Tokuno, K.; Hasegawa, M.; Linert, W.; Mereiter, K. *Acta Crystallogr.* **2010**, E66, m399–m400. (b) Hartdegen, V.; Klapotke, T. M.; Sproll, S. M. *Z. Naturforsch.* **2009**, 64b, 1535–1541.

(49) Void areas [\AA^3] per one anion calculated by PLATON in different temperatures for 1: 293 K, 92; 230, 89, 185 K, 86; 155 K, 82; 100 K, 77; 230 K, 89 and for 2: 293 K, 87; 225 K, 86; 195 K, 83; 190 K, 76; 185 K, 76, 100 K, 75; 225 K, 87.

(50) Michael, D.; Mingos, P.; Rohl, A. L. *J. Chem. Soc., Dalton Trans.* **1991**, 3419–3425.